

## OPTICS AND SPECTROSCOPY

### QUANTUM-CHEMICAL STUDY OF THE NATURE OF ELECTRONICALLY EXCITED STATES OF HYDROXYAROMATIC COMPOUNDS

E. N. Bocharnikova, O. N. Tchaikovskovskaya, and V. Ya. Artyukhov

UDC 539.194:535.37

*Spectroscopy methods make it possible to record the features of specific photo-induced processes occurring inside and between molecules and, moreover, chemical and structural changes of such objects can be monitored and controlled interactively with the help of luminescent molecular probes with known spectral properties. In order to solve the general fundamental problem of establishing the connection of the photophysical and spectral-luminescent properties of organic molecules with their structure, a comparative analysis was made of the nature of electronically excited states and photoprocesses occurring in phenol and its related compounds (*p*-cresol and bisphenol A). To understand the mechanism of forming the absorption and fluorescence spectra of hydroxyaromatic compounds, the electronically excited states of the molecules under study are presented and analyzed together with the localization of molecular orbitals and the local minima of the electrostatic potential. The results of these calculations have shown that the proton-acceptor ability of isolated molecules is associated with an excess of electron density on oxygen atoms and increases in the series: phenol < *n*-cresol < bisphenol A. This order is maintained when excited to the  $S_1$  and  $S_2$  states. At the same time, the proton-acceptor ability of phenols decreases in comparison with the ground state. The consequence of the non-planar structure of the bisphenol A (BPA) molecule is the mixed orbital nature of the electronically excited states. The non-planar structure of the BPA leads to an increase in the spin-orbit interaction and in the intercrossing conversion constant between  $S_1(\pi\pi^*)$  and  $T_6(\pi\sigma^*)$  states compared to phenol.*

**Keywords:** phenol, *p*-cresol, bisphenol A, absorption, photophysical processes, quantum-chemical calculation.

## INTRODUCTION

One of the fundamental problems of modern photonics of multiatomic organic compounds is the establishment of the dependence of spectral luminescent and photochemical properties of multiatomic molecules on their electronic structure, nature of the electronically excited states, and intermolecular interactions. Its solution is urgent now for such related branches of science, as biophysics, biochemistry, synthesis of medical preparations, and ecology. Photoexcitation of molecules changes significantly their electronic structure and reactivity [1, 2]. In case of photochemical reactions, a solvent can strongly affect the reaction rate and direction. This is due to the possibility of forming weak complexes with the solvent that can change the relative positions of the electronically excited states of the dissolved molecule. This is manifested primarily through a dependence of the absorption and fluorescence spectra on the nature of the solvent. The photophysical processes in a molecule can often change the rate constants of radiative and non-radiative processes and, as a consequence, the quantum yields of photochemical reactions.

---

National Research Tomsk State University, Tomsk, Russia, e-mail: bocharnikova.2010@mail.ru; tchon@phys.tsu.ru; victor.art@rambler.ru. Translated from *Izvestiya Vysshikh Uchebnykh Zavedenii, Fizika*, No. 9, pp. 144–150, September, 2019. Original article submitted May 18, 2019.

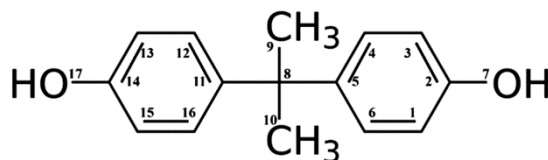


Fig. 1. Structural BPA formula.

The phenol molecule is a classical object on the example of which the special features of spectral manifestations of intermolecular interactions of resonant and inductive resonant natures [1] and of hydrogen bonds were studied [2]. Bisphenol A (4,4'-dihydroxy-2,2-diphenylpropane (BPA)) is a chemical substance belonging to the class of phenols widely used as monomers for production of epoxy resin, polycarbonate, unsaturated polyester styrene resin, and antipyrine [3]. Final industrial products are used as lids for cans, powder paints, additives to thermal paper, tooth fillings, and antioxidants in plastics. BPA is one of the chemical substances with high production volume: its annual production volume all over the world exceeds 8 billion pounds. Because of a high level of consumption and an adverse effect on the state of wild nature, BPA is well known as one of xenobiotics of considerable recent public interest. BPA possesses estrogen activity and is classified as a compound destroying endocrine system. This disturbing situation has led to a study of stimulated or natural BPA degradation, including its photochemical decomposition in waters of various types [4, 5].

With the development of high resolution technology, the quantum yield of triplets was measured for phenolic compounds [6]. Based on an analysis of the experimental photophysical parameters, Grabner *et al.* [6] proposed the mechanism of deactivation of the lowest singlet phenol states in nonpolar solvents. Discussing methods of deactivation of the state  $S_1$  of phenol and its substitutes, the authors pointed out that the lifetime of the fluorescent state was about 2 ns, and methylation did not change it. The quantum fluorescence yield did not exceed 8 %. The conversion  $S_1 \approx T_1$  was more significant, and this channel was influenced by the solvent polarity. The efficiency of the process  $S_1 \approx T_1$  did not exceed 18 %, and was not a priority for deactivation of the fluorescent state. Experimental results also demonstrated that the radical mechanism of phenol decay was insignificant. The quantum yield of all channels that were not taken into account was approximately 50 %. The authors, referring to experiment with a jet [7], proposed to refer the disregarded channels to internal conversion, indicating that the conversion  $S_1 \approx S_0$  can be the main channel for deactivation of the state  $S_1$  in nonpolar solvents due to a change in the molecule geometry during excitation.

To develop a high-sensitive fluorescent method of analysis and monitoring of the spectral properties of aromatic compounds, it is necessary to establish interrelation of the change of degradation channels for the excitation energy of molecules with the specific features of their composition, the spectral range of excitation sources, and the solvent. This research is aimed at experimental and theoretical study of the influence of the molecular structures in the series: phenol, 4-metilfenol (*n*-cresol), and bisphenol A on the nature of the electronically excited states.

## OBJECTS AND METHODS OF RESEARCH

Phenol, *n*-cresol, and 4,4'-dihydroxy-2,2-diphenylpropane (bisphenol A or BPA) were chosen as objects of research. The structural BPA formula is presented in Fig. 1.

The spectral and luminescent characteristics of phenols in nonpolar solvents were recorded on an SM 2203 spectrofluorimeter ("SOLAR," Belarus) [8]. The absorption and fluorescence spectra were recorded with concentration of examined molecules of  $10^{-5}$  M in a quartz cell 1 cm thick. The derivative spectrophotometry method was used to select the bands manifested in the absorption spectrum only as latent maxima and fuzzy kinks. This method is based on the same principles as the conventional spectrophotometry; however, as an analytical signal, the *n*th order derivative of the optical density (typically with respect to the wavelength) rather than the optical density itself are employed. Differentiation of the spectrum allows the position of the absorption band maximum to be determined more exactly,

TABLE 1. Experimental and Theoretical Positions of the Phenol, *n*-Cresol, and BPA Absorption Bands

Serial No.	Transition	Phenol		<i>n</i> -Cresol		Bisphenol A	
		Experiment <sup>1</sup> , cm <sup>-1</sup>	Calculation, cm <sup>-1</sup> (nature)	Experiment, cm <sup>-1</sup>	Calculation, cm <sup>-1</sup> (nature)	Experiment, cm <sup>-1</sup>	Calculation, cm <sup>-1</sup>
1	$S_0 \rightarrow S_1$	37800 <sup>2</sup>	38100 ( $\pi\pi^*$ )	36100	36300 ( $\pi\pi^*$ )	36200	35143
2		36830 <sup>2</sup>					
3		35900 <sup>2</sup>					
4	$S_0 \rightarrow S_2$	Unidentified	44600 ( $\pi\pi^*$ )	45500	42400 ( $\pi\sigma^*$ )	41200	35606
5	$S_0 \rightarrow S_3$		48300 ( $\pi\pi^*$ )		43300 $\pi\pi^*$		36148
6	$S_0 \rightarrow S_4$		49800 ( $\pi\pi^*$ )		37946		
7	$S_0 \rightarrow S_5$		38510				
8	$S_0 \rightarrow S_6$		40342				
9	$S_0 \rightarrow S_7$		42572				
10	$S_0 \rightarrow S_8$		45500	44180			
11	$S_0 \rightarrow S_9$		44889				
12	$S_0 \rightarrow S_7$		45319				

Notes. Here <sup>1</sup> indicates the hexane solvent, and <sup>2</sup> indicates the maxima of the vibronic transitions of the first absorption band.

narrows bands, and allows substances whose initial spectra are partially superimposed to be identified. Using this method, we succeeded in subdivision of the long-wavelength absorption band of phenols in solvents into absorbing centers.

Theoretical studies of the chosen compounds were performed using the software package based on the semiempirical INDO method with special spectroscopic parameterization [9]. The procedures of estimating the rate constants of the photoprocesses are described in [10, 11]. The software package allowed the following characteristics of the electronic states of multiatomic molecules to be determined: the energy and the nature of the molecular orbitals, the energy and the wave functions of the singlet and triplet electronically excited states, the oscillator forces and polarization of electronic transitions, the electron density distribution for atoms and molecular bonds, the dipole moments of the ground and excited states, and the absorption and fluorescence spectra. The geometry was optimized by the quantum-chemical method *AustinModel1 (AMI)* [12]. The exact structural BPA parameters (bond lengths, valence, and torsion angles) were unknown; therefore, the geometry of the ground state was optimized by the method of molecular mechanics (*MM2 Chem Office*) [13]. The wave functions calculated by the INDO method were used for calculation of the molecular electrostatic potential (MESP) [14, 15] with the help of which the points of maximum electrostatic interaction of spatially distributed charge of the molecule and the unit positive point charge were estimated. The change of the strength of this interaction and of the place of its maximum manifestation allowed us to determine the change in the solvate molecule shell during electronic excitation.

## RESULTS AND DISCUSSION

The long-wavelength absorption bands of phenol in hexane are structurized (Table 1). According to the results of quantum-chemical calculations [1], absorption in this range is caused by the single electronic transition  $S_0 \rightarrow S_1$  of the  $\pi\pi^*$ -type; therefore, and the observed band structure demonstrates its vibrational structure. In the electronic absorption spectrum of phenol in the range up to 50000 cm<sup>-1</sup>, two absorption bands with maxima at ~37000 and 47400 cm<sup>-1</sup> were distinguished. The results of quantum-chemical calculations of isolated phenol molecules showed that in the range up to 50000 cm<sup>-1</sup>, the molecular orbitals of the  $\sigma$ -type, localized on the OH bond (Table 1) do not participate in the formation of the wave functions of the excited states. The incorporation in the benzene ring of the CN<sub>3</sub> group leads to a decrease in the calculated energy of electronic transitions, a bathochromic shift of the band maxima in

TABLE 2. Values of the Bond Lengths, Valences, and Torsion Angles for the Geometry of the Isolated BPA Molecule Optimized by the *AM1* Method

Serial No.	Bond between atoms		Bond length, Å	Valence angle	Torsion angle
1	1	2	1.501	88.059	204.571
2	2	3	1.333	120.552	266.705
3	3	4	1.429	117.911	359.408
4	4	5	1.431	122.643	0.263
5	5	6	1.440	117.842	0.239
6	2	7	1.343	118.656	86.550
7	5	8	1.521	118.315	179.339
8	8	9	1.528	107.906	290.220
9	8	10	1.529	110.285	172.947
10	8	11	1.501	117.556	56.573
11	11	12	1.417	122.999	263.697
12	12	13	1.423	121.833	176.285
13	13	14	1.322	120.169	348.034
14	14	15	1.507	115.155	20.929
15	15	16	1.341	123.030	348.762
16	14	17	1.352	118.395	189.284

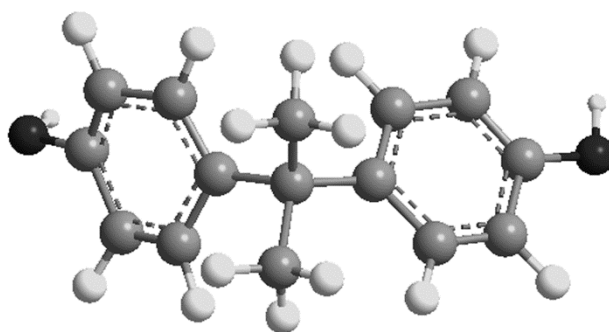


Fig. 2. Optimized structure of the molecule studied by the *AM1* method.

the long-wavelength and middle regions of the spectrum, and an increase in the long-wavelength absorption band intensity. In the long-wavelength band of the *n*-cresol, the vibronic levels were manifested in the form of two kinks. The band was formed by the single electronic transition  $S_0 \rightarrow S_1$  of the  $\pi\pi^*$ -type. In the middle range of the spectrum, an electronic transition of the  $\pi\sigma^*$ -type arises. As to the electronic transitions of phenol and *n*-cresol in the region of the spectrum around  $\sim 50000 \text{ cm}^{-1}$ , they were localized only on carbon atoms of the aromatic ring of molecules. According to the experimental results, the maximum of the fluorescence bands of phenol and *n*-cresol in hexane is at  $\sim 33000 \text{ cm}^{-1}$ .

Values of the bond lengths, valences, and torsion angles (optimized geometry) given in Table 2 indicate a non-planar character of the BPA molecule (Fig. 2). The experimental maximum of the long-wavelength absorption band of BPA in hexane was observed at 274 nm ( $\sim 36500 \text{ cm}^{-1}$ ), and the maximum of the fluorescence band was at 298 nm ( $\sim 33560 \text{ cm}^{-1}$ ). The calculated absorption spectrum of the isolated BPA molecule is presented in Tables 1 and 3. The experimental long-wavelength absorption band of BPA in hexane corresponded to the energy and the oscillator force of the calculated  $S_0 \approx S_3$  transition of the  $\pi\pi^*$ -type forming the absorption in the long-wavelength range of the electronic spectrum of the isolated molecule.

TABLE 3. Nature of Electronically Excited BPA States

State	Characteristic*			
	$E_n, \text{cm}^{-1}$	$f$	Polarization of the $S_0 \rightarrow S_n$ transition	$\mu_n, D$
$S_1 (\pi\pi^*)$	35143	0.063	$X$	3.12
$S_2 (\pi\pi^*)$	35606	0.053	$X$	2.93
$S_3 (\pi\pi^*)$	36148	0.121	$Y$	6.8
$S_4 (\pi\pi^*)$	37946	0.005	$X$	4.86
$S_5 (\pi\pi^*)$	38510	0.402	$Y$	2.12
$S_6 (\pi\pi^*)$	40342	0.233	$X$	2.03
$S_7 (\pi\sigma^*)$	42572	0.004	$Z$	2.96
$S_8 (\pi\sigma^*)$	44180	0.002	$Z$	2.55
$S_9 (\pi\sigma^*)$	44889	0.135	$Z$	3.74
$S_{10} (\pi\sigma^*)$	45319	0.151	$Z$	2.66
$T_1 (\pi\pi^*)$	23955	0.152	$Y$	2.28
$T_2 (\pi\pi^*)$	24107	0.187	$X$	2.04
$T_3 (\pi\sigma^*)$	32190	0.005	$X, Y$	5.9
$T_4 (\pi\pi^*)$	32627	0.527	$X$	2.3
$T_5 (\pi\sigma^*)$	32942	0.317	$Z$	2.87
$T_6 (\pi\sigma^*)$	34325	0.256	$Z$	3.57
$T_7 (\pi\pi^*)$	36351	0.554	$X$	2.24
$T_8 (\pi\pi^*)$	38212	0.633	$Y$	2.85
$T_9 (\pi\sigma^*)$	39776	0.005	$Z$	2.54
$T_{10} (\pi\sigma^*)$	41333	0.052	$X, Z$	3.74

Notes.  $*E_i$  and  $f$  here indicate the energy and the oscillator force of the  $S_0 \rightarrow S_n$  and  $T_0 \rightarrow T_n$  transitions, and  $\mu_i$  denotes the dipole moment of the molecule in the excited state.

Figure 3 shows the calculated energy level diagrams of the examined molecules. An analysis of the rate constants of photophysical processes allowed us to conclude the following on the formation of the fluorescent properties of phenols. Upon excitation of phenol and *n*-cresol to the long-wavelength absorption band, the absorbed energy deactivates through two channels – the radiative channel and the channel of singlet-triplet conversion  $S_1(\pi\pi^*) \gtrsim T_3(\pi\pi^*)$ . The process of internal conversion  $S_1 \rightarrow S_0$  has low efficiency. Upon excitation to the state  $S_2$ , the quantum fluorescence yield remained the same, as upon excitation to the state  $S_1$ , since the efficiencies of the internal conversion  $S_2(\pi\pi^*) \gtrsim S_1(\pi\pi^*)$  and of the singlet-triplet  $S_2(\pi\pi^*) \gtrsim T_4(\pi\sigma^*)$  and  $T_3(\pi\pi^*) \gtrsim S_1(\pi\pi^*)$  conversions were high. The excitation energy deactivated through channels of the non-radiative conversion to the state  $S_1$  due to the spin-orbit bond between the states  $S_1$ ,  $T_3$ , and  $T_4$ . For the *n*-cresol molecule, the process of internal conversion in the channel  $T_4 \gtrsim T_3$  was delayed by an order of magnitude compared to phenol (Fig. 3).

A consequence of the non-planar structure of the BPA molecule (Table 3 and Fig. 2) was the mixed character of the orbital nature of the electronically excited states. Therefore, the nature of the excited state referred to a certain orbital type indicated in Table 2 testified only to its predominant contribution. The BPA absorption spectrum in the long-wavelength and middle ranges of the spectrum was shifted toward lower energies, the intensity of electronic transitions increased, and the orbital nature of the transitions forming absorption bands remained unchanged. The non-planar BPA structure led to the fact that when going from phenol to BPA, the spin-orbit interaction intensified and the constant of intercrossing conversion between the  $S_1(\pi\pi^*)$  and  $T_6(\pi\sigma^*)$  states of BPA increased by two orders of

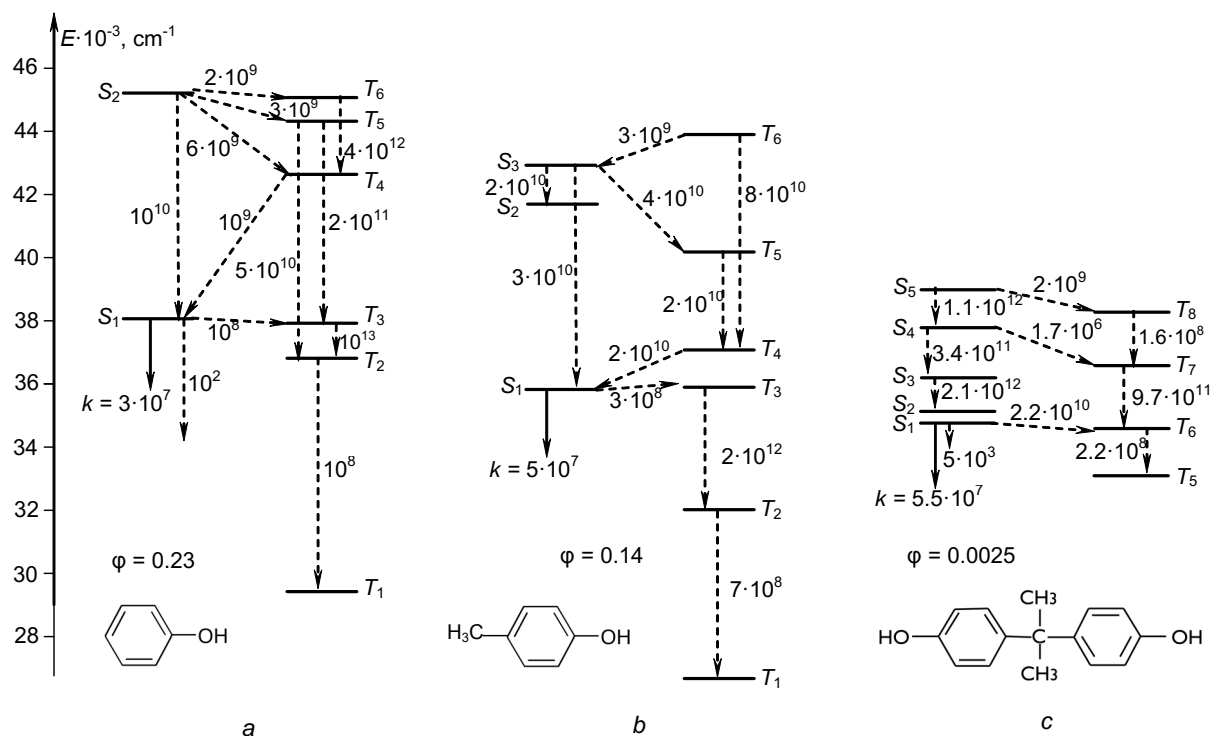
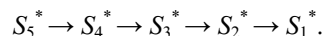


Fig. 3. Electronically excited states and photoprocesses in isolated molecules: a) phenol, b) *n*-cresol, and c) bisphenol A. The rate constants of the photoprocesses are given in  $\text{s}^{-1}$ . Here  $\phi$  are the calculated quantum fluorescence yields.

magnitude compared to phenol. From Fig. 3 it can be seen that because of the high efficiency of the non-radiative  $S$ - $S$  conversion, the channel of energy degradation upon excitation of the BPA molecule to the region above  $38000 \text{ cm}^{-1}$  has the following path:



Then the excitation energy degrades non-radiatively through the channel  $S_1 \approx T_6$  and further through the  $T$ - $T$  conversion channel (Fig. 3) upon excitation both to the region above  $35000 \text{ cm}^{-1}$  and to the high-energy states (above  $45000 \text{ cm}^{-1}$ ). It should be noted that the close arrangement of the  $S_5$  state of the  $\pi\pi^*$ -type and of the triplet  $T_8$  state of the  $\pi\sigma^*$ -type can lead to the excitation energy transfer to the system of the electronically excited triplet states. The photophysical processes proceeding in BPA led to a low quantum fluorescence yield (the calculated yield was  $\phi = 0.003$ ). The theoretical value had the same order of magnitude as the experimental value  $\phi = 0.001$ .

Our calculations demonstrated that the most part of the negative charge in phenol molecules was concentrated on the oxygen atom near which two local MESP minima ( $-207$ ) were localized symmetric about the long axis of the molecule. This indicates the possibility of simultaneous attachment of two water molecules, that is, the formation of the complex 1:2 was most probable near the oxygen atom. Therefore, the proton acceptor ability of the isolated phenol molecule was related with the excessive electronic density on the oxygen atom of the OH group and was maximal in the ground state. The electronic excitation to the states  $S_1$  or  $S_2$  decreased the proton acceptor ability of phenol (the MESP was equal to  $-207$  in the state  $S_0$  and to  $-127$  in the states  $S_1$  and  $S_2$ ) and *n*-cresol (the MESP was equal to  $-267$  in the state  $S_0$  and  $-197$  in the states  $S_1$  and  $S_2$ ). This was a consequence of electronic density transfer from the oxygen atom of the OH group to the aromatic ring. The electronic density was transferred through the  $\pi$ -system of the molecule. As

TABLE 4. Effective Charges on Atoms of the BPA Molecule in the States  $S_0$  and  $S_1$ 

Serial No.	Atomic number	Effective charges on the atoms	
		State $S_0$	State $S_1$
1	1	-0.027	-0.039
2	2	0.203	0.238
3	3	-0.057	-0.042
4	4	-0.053	-0.051
5	5	-0.015	0.034
6	6	-0.027	-0.059
7	7	-0.313	-0.262
8	8	0.049	0.053
9	9	0.008	0.015
10	10	-0.002	0.000
11	11	0.001	0.009
12	12	-0.065	-0.082
13	13	-0.022	-0.059
14	14	0.200	0.207
15	15	-0.034	-0.078
16	16	-0.045	-0.099
17	17	-0.350	-0.337

a result, a weak excess of the negative charge arose over the plane of the aromatic ring of the molecules. The most probable place of proton attachment to the phenol or *n*-cresol molecule is the oxygen atom of the OH group. It should be noted that the presence of the substitute of the CH<sub>3</sub> group of the *n*-cresol molecule increased the proton acceptor ability of the oxygen atom compared to phenol [16].

The proton acceptor ability of the isolated BPA molecule was also associated with the excess in the electronic density on oxygen atoms of OH groups (atoms 7 and 17 in Table 4). The electronic excitation of the state  $S_1$  decreased the proton acceptor ability of BPA as a result of the electronic density transfer from the oxygen atoms to the carbon atoms of the aromatic rings.

## CONCLUSIONS

As a result of our study, we have experimentally and theoretically established the following.

1. The proton acceptor ability of the isolated molecules is associated with the excess of the electronic density on the oxygen atoms; it increased in the series phenol < *n*-cresol < bisphenol A. This order remained unchanged upon excitation to the states  $S_1$  and  $S_2$ . Moreover, the proton acceptor ability of phenols in the electronically excited states decreased compared to the ground state.

2. Incorporation of substitutes in the phenol structure increased the efficiency of the non-radiative  $S$ - $S$  processes in the series phenol < *n*-cresol < bisphenol A.

3. The process of the  $S$ - $T$  conversion is the main channel of degradation of the excitation energy ( $k_{ST} \sim 2.2 \cdot 10^{10} \text{ s}^{-1}$ ) in BPA.

The results were obtained within the framework of the State Assignment of the Ministry of Education and Science of the Russian Federation (Project No. 4.6027.2017/8.9) and of the Program for Increasing the Competitiveness of TSU among the Leading World Scientific Educational Centers.

## REFERENCES

1. Yu. P. Morozova, O. K. Tchaikovskaya, and Yu. N. Vasil'eva, *Zh. Fiz. Khim.*, **72**, No. 2, 272–279 (1998).
2. K. Fuke and K. Kaya, *Chem. Phys. Lett.*, **94**, No. 1, 97–103 (1983).
3. M. Tohmé, S. M. Prud'homme, A. Boulahtouf, *et al.*, *The FASEB J.*, **28**, No. 7, 312–433 (2014).
4. É. M. Sokolov, L. É. Sheinkman, and D. V. Dergunov, *Water: Chem. Ecol.*, No. 4, 26–32 (2012).
5. G. G. Matafonova, N. I. Vorob'eva, and V. B. Batoev, *Izv. Vyssh. Uchebn. Zaved. Khim. Khim. Tekhnol.*, **57**, No. 7, 118–121 (2014).
6. G. Grabner, G. Kohler, G. Marconi, *et al.*, *J. Phys. Chem.*, **94**, 3609–3613 (1990).
7. G. Kohler and N. Getoff, *J. Chem. Soc. Faraday Trans.*, **72**, No. 10, 2101–2106 (1976).
8. GOST 12997-84 “SSI Products. General Specifications.” Specifications TU BY 100424659.013-2006 “Spektrofluorimeter SM 2203.”
9. V. Ya. Artyukhov and A. I. Galeeva, *Russ. Phys. J.*, **29**, No. 11, 949–952 (1986).
10. V. A. Blatov, A. P. Shevchenko, and E. V. Peresypkina, *Semiempirical Computational Methods of Quantum Chemistry: A Textbook [in Russian]*, Publishing House “Univer-Group,” Samara (2005).
11. V. Ya. Artyukhov, N. N. Kopylova, L. G. Samsonova, *et al.*, *Russ. Phys. J.*, **51**, No. 10, 1097–1111 (2008).
12. M. Dewar and R. Dogerty, *Molecular Orbital Perturbation Theory in Organic Chemistry [Russian translation]*, Mir, Moscow (1977).
13. <http://www.cambridgesoft.com>.
14. E. Scroco and J. Tomasi, *Adv. Quant. Chem.*, **11**, 115–193 (1978).
15. V. Ya. Artyukhov, *J. Struct. Chem.*, **19**, No. 3, 364–368 (1978).
16. O. N. Tchaikovskaya, T. V. Sokolova, and I. V. Sokolova, *Zh. Prikl. Spekr.*, **72**, No. 2, 165–170 (2005).